Article

Cell

CDK7-Dependent Transcriptional Addiction in Triple-Negative Breast Cancer

Graphical Abstract

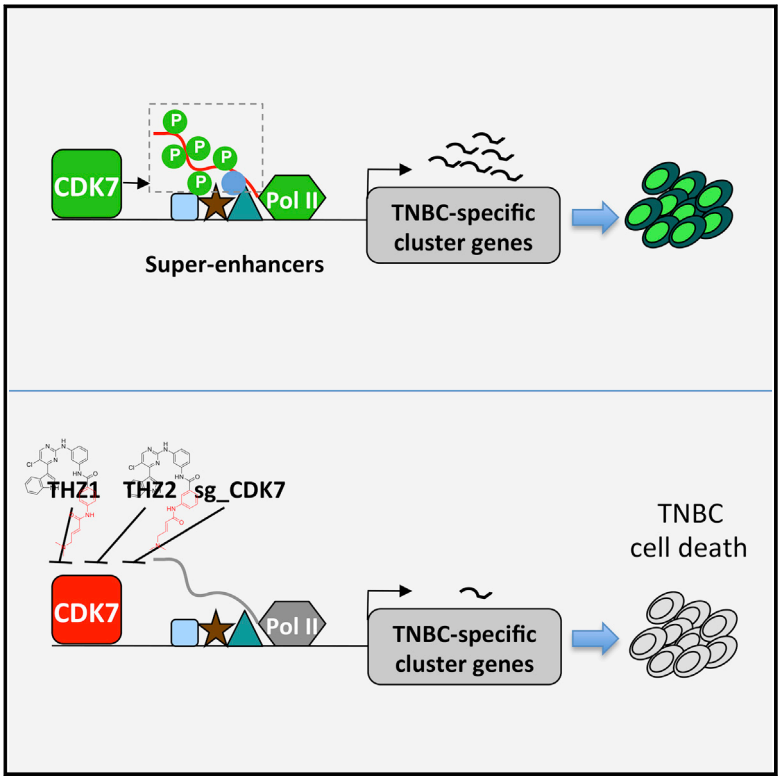

Authors

Yubao Wang, Tinghu Zhang, Nicholas Kwiatkowski, ..., Richard A. Young, Nathanael S. Gray, Jean J. Zhao

Correspondence

nathanael_gray@dfci.harvard.edu (N.S.G.), jean_zhao@dfci.harvard.edu (J.J.Z.)

In Brief

A potential therapy for triple-negative breast cancer is suggested by its strong dependence on the transcriptional kinase CDK7 and the cluster of genes the kinase regulates.

Highlights

- Triple-negative breast cancer (TNBC) cells are highly dependent on CDK7
- CRISPR/Cas9-mediated gene editing shows selective dependency of TNBC on CDK7
- CDK7 activity is critical for the expression of a set of genes essential for TNBC
- A covalent CDK7 inhibitor blocks tumor growth in patient-derived xenografts of TNBC

Accession Numbers

GSE69107

Wang et al., 2015, Cell *163*, 174–186
September 24, 2015
http://dx.doi.org/10.1016/j.cell.2015.08.063

CellPress

Cell

Article

CDK7-Dependent Transcriptional Addiction in Triple-Negative Breast Cancer

Yubao Wang,[1,2,7] Tinghu Zhang,[1,2,7] Nicholas Kwiatkowski,[3,7] Brian J. Abraham,[3] Tong Ihn Lee,[3] Shaozhen Xie,[1,2] Haluk Yuzugullu,[1,2] Thanh Von,[1,2] Heyuan Li,[1] Ziao Lin,[1] Daniel G. Stover,[4] Elgene Lim,[4] Zhigang C. Wang,[1,5] J. Dirk Iglehart,[1,5] Richard A. Young,[3,6,8] Nathanael S. Gray,[1,2,8,*] and Jean J. Zhao[1,2,8,*]

[1]Department of Cancer Biology, Dana-Farber Cancer Institute, Boston, MA 02115, USA
[2]Department of Biological Chemistry and Molecular Pharmacology, Harvard Medical School, Boston, MA 02115, USA
[3]Whitehead Institute for Biomedical Research, 9 Cambridge Center, Cambridge, MA 02142, USA
[4]Department of Medical Oncology, Dana-Farber Cancer Institute, Boston, MA 02115, USA
[5]Department of Surgery, Brigham and Women's Hospital, Boston, MA 02115, USA
[6]Department of Biology, Massachusetts Institute of Technology, Cambridge, MA 02139, USA
[7]Co-first author
[8]Co-senior author
*Correspondence: nathanael_gray@dfci.harvard.edu (N.S.G.), jean_zhao@dfci.harvard.edu (J.J.Z.)
http://dx.doi.org/10.1016/j.cell.2015.08.063

SUMMARY

Triple-negative breast cancer (TNBC) is a highly aggressive form of breast cancer that exhibits extremely high levels of genetic complexity and yet a relatively uniform transcriptional program. We postulate that TNBC might be highly dependent on uninterrupted transcription of a key set of genes within this gene expression program and might therefore be exceptionally sensitive to inhibitors of transcription. Utilizing kinase inhibitors and CRISPR/Cas9-mediated gene editing, we show here that triple-negative but not hormone receptor-positive breast cancer cells are exceptionally dependent on CDK7, a transcriptional cyclin-dependent kinase. TNBC cells are unique in their dependence on this transcriptional CDK and suffer apoptotic cell death upon CDK7 inhibition. An "Achilles cluster" of TNBC-specific genes is especially sensitive to CDK7 inhibition and frequently associated with super-enhancers. We conclude that CDK7 mediates transcriptional addiction to a vital cluster of genes in TNBC and CDK7 inhibition may be a useful therapy for this challenging cancer.

INTRODUCTION

Recent advances in genomic sequencing have led to an unprecedented understanding of the genetics of tumor heterogeneity (Fisher et al., 2013). For a number of cancers, this has led to the discovery of "driver" oncogenes such as mutant BRAF, EGFR, and EML4-ALK, which has informed rational drug development strategies (Chin et al., 2011). For other tumors, however, sequencing has only revealed a striking level of heterogeneity and has not resulted in the identification of clear driver mutations (Cancer Genome Atlas Research Network, 2011, 2012). Despite this genetic heterogeneity, a number of these tumors can be readily identified based upon their gene expression programs (Hoadley et al., 2014). We hypothesized that, despite the genetic heterogeneity, maintenance of these uniform gene expression programs might require continuous active transcription and therefore be more sensitive to drugs that target transcription.

We evaluated this hypothesis in the context of triple-negative breast cancer (TNBC) because this subtype is characterized by high genetic complexity (Abramson et al., 2015; Cancer Genome Atlas Network, 2012) and has a characteristic gene expression program (Parker et al., 2009; Perou et al., 2000). Compared to hormone receptor (estrogen and/or progesterone receptor)-positive (ER/PR+) breast cancer, TNBC demonstrates a higher level of genetic complexity, as indicated by a higher rate of point mutation, gene amplification, and deletion (Cancer Genome Atlas Network, 2012). Notably, TNBC lacks a common genetic alteration except mutations of tumor suppressor genes such as INPP4B, PTEN, and TP53 (Abramson et al., 2015; Andre et al., 2009; Cancer Genome Atlas Network, 2012; Gewinner et al., 2009; Shah et al., 2012), a situation that has limited the development of "targeted" therapies. The highly aggressive nature of TNBC and the lack of effective therapeutics make this disease a high priority for discovery biology efforts.

Targeting gene transcription for cancer therapy has long been considered difficult, due to a presumably universal role of transcription in non-malignant cells or tissues, and consequently, pharmacologic inhibition of general transcriptional machinery might lack selectivity for cancer cells and cause intolerable toxicity. Recent studies, however, have challenged this paradigm and found that transcription of certain genes is disproportionately sensitive to inhibition of transcription (Dawson et al., 2011; Delmore et al., 2011; Chapuy et al.; 2013; Chipumuro et al., 2014; Christensen et al., 2014; Kwiatkowski et al., 2014; Zuber et al., 2011). Those genes, often encoding oncogenic drivers with short mRNA and protein half-lives (e.g., MYC, MYCN, and RUNX1), have a striking dependence on continuous active transcription, thereby allowing for highly selective effects before "global" downregulation of transcription is achieved. The continuous active transcription of these genes in cancer cells is often driven by exceptionally large clustered enhancer regions, called super-enhancers, that are densely occupied by

transcription factors and co-factors (Hnisz et al., 2013, 2015; Lovén et al., 2013).

The control of gene transcription involves a set of cyclin-dependent kinases (CDKs), including CDK7, CDK8, CDK9, CDK12, and CDK13, that play essential roles in transcription initiation and elongation by phosphorylating RNA polymerase II (RNAPII) and other components of the transcription apparatus (Akhtar et al., 2009; Larochelle et al., 2012; Zhou et al., 2012). We recently discovered a selective CDK7 inhibitor, THZ1, that covalently binds to CDK7 and suppresses its kinase activity with an unanticipated level of selectivity based upon modification of a unique cysteine residue (Kwiatkowski et al., 2014). We further identified a therapeutic effect of CDK7 inhibition in several types of cancer, including MYCN-amplified neuroblastoma, small-cell lung cancer, and T cell acute lymphoblastic leukemia (Chipumuro et al., 2014; Christensen et al., 2014; Kwiatkowski et al., 2014). Here, we report that TNBC demonstrates a profound dependence on CDK7. We further identified an "Achilles cluster" of TNBC genes that require CDK7 to maintain expression and that apparently mediate the extreme sensitivity of TNBC to CDK7 inhibition.

RESULTS

Exceptional Sensitivity of TNBC Cells to Covalent Inhibition of CDK7

To investigate whether the proliferation of TNBC cells is sensitive to CDK7 inhibition, we treated triple-negative or ER/PR+ breast cancer cell lines with increasing concentrations of THZ1. While ER/PR+ cells were largely unaffected by treatment of THZ1 at micromolar doses, triple-negative breast cancer cells were highly sensitive to CDK7 inhibition, with cell proliferation effectively suppressed by low nanomolar concentrations of THZ1 ($IC_{50} < 70$ nM) (Figures 1A and 1B). In contrast to the extreme sensitivity to THZ1, TNBC cells were more resistant to a non-cysteine reactive analog of THZ1 (THZ1-R) (Kwiatkowski et al., 2014) (Figure S1A), suggesting that the unique characteristic of THZ1 in covalently binding to its target determines its antiproliferative potency.

To understand the mechanism underlying the highly selective effect of THZ1, we next proceeded to test whether CDK7 is equally inhibited in both triple-negative and ER/PR+ breast cancer cells. CDK7 is implicated in regulating the phosphorylation of the carboxyl-terminal domain (CTD) of RNAPII at multiple sites (Ser 2, 5, and 7) either directly or via phosphorylating and activating other CDKs (Akhtar et al., 2009; Glover-Cutter et al., 2009; Larochelle et al., 2012; Zhou et al., 2012). We exposed cells to increasing doses of THZ1 or THZ1-R and found that, in both triple-negative and ER/PR+ breast cancer cells, CTD phosphorylation at S2, S5, and S7 was effectively suppressed by THZ1 but not the inactive THZ1-R (Figures 1C and S1B). The similar effects on CTD phosphorylation by THZ1 indicates that CDK7 is similarly targeted in both drug-sensitive and -resistant cells; thus, TNBC cells appear to be far more dependent on the activity of CDK7 than ER/PR+ breast cancer cells.

We further found that CDK7 inhibition efficiently induced apoptotic cell death in TNBC cells, indicated by the induced cleavage of PARP and Caspase 3 (Figure 1D). In line with the differential response to CDK7 inhibition, cell death was not observed in ER/PR+ breast cancer cells treated with THZ1 (Figure 1D). Consistent with previous studies, THZ1 treatment also failed to induce cell death in non-transformed human cell lines (BJ fibroblasts and retinal pigment epithelial cells, RPE-1) (Figure 1D) (Kwiatkowski et al., 2014). Notably, RNAPII CTD phosphorylation was suppressed by THZ1 in all of these cell lines (Figure 1D) and thus did not correlate with the cell fate, again indicating an exceptional dependence on CDK7-regulated pathways in TNBC cells.

In addition to regulating RNAPII CTD phosphorylation, CDK7 is a component of CDK-activating kinase (CAK), which is thought to phosphorylate and activate all CDKs, including cell-cycle CDKs (Schachter and Fisher, 2013). Indeed, CDK7 has been implicated in phosphorylating CDK1 and regulating mitosis (Larochelle et al., 2007), and THZ1 treatment has been shown to induce a G2/M arrest in neuroblastoma cells with MYCN amplification (Chipumuro et al., 2014). Surprisingly, THZ1 treatment did not alter the cell cycle in TNBC cells (Figure S1C). To further investigate whether mitosis is impaired by CDK7 inhibition, we utilized live-cell imaging to observe the progression of mitosis. We found that mitosis of TNBC cells (MDA-MB-468) progressed normally in the presence of THZ1 (Figure S1D and Movie S1 and S2). The duration of time from nuclear envelope breakdown (NEBD) to anaphase onset was not significantly changed by THZ1 treatment (Figure S1E). Despite a lack of mitotic arrest by THZ1, cell death was efficiently induced (Figures S1D and S1F and Movie S1). Therefore, the sensitivity of TNBC cells to CDK7 inhibition is likely not derived from a role of CDK7 in directly regulating cell-cycle-related CDKs.

Next, we investigated whether the anti-proliferative effects displayed by THZ1 in established TNBC cell lines would translate to primary TNBC samples. To address this, we performed primary culture of tumor cells from patient-derived xenografts (PDX) of TNBC and treated these cells with THZ1. In three independent patient-derived TNBC cultures, THZ1 effectively reduced cell viability ($IC_{50} < 100$ nM) (Figure 1E). Consistent with our findings obtained from established cancer cell lines, we observed that two ER/PR+ primary cultures were largely insensitive to THZ1 (Figures 1E and 1F). Furthermore, treatment of primary TNBC cells with THZ1 led to suppressed RNAPII CTD phosphorylation and induction of apoptotic cell death (Figure 1G). Given that the primary samples were derived from patients with TNBC who had progressed on multiple lines of chemotherapies, our data indicate that CDK7 inhibition may provide an effective therapeutic option for patients with this aggressive disease.

An Analog of THZ1 with Improved Pharmacokinetics

Despite the high anti-proliferative potency of THZ1 in primary TNBC cells, the stability of THZ1 in vivo (T1/2 of 45 min in mouse plasma) limits its utility for in vivo investigations. We therefore modified the structure of THZ1 by altering the regiochemistry of the acrylamide on THZ1 from 4-acrylamide-benzamide to 3-acrylamide-benzamide, giving rise to an analog THZ2 (Figure 2A). THZ2 had significantly improved pharmacokinetic features, with a 5-fold improved half-life in vivo (Figure 2B). Similar to THZ1, THZ2 selectively targeted CDK7 (Figure 2C and Table S1) and potently inhibited the growth of triple-negative, but not ER/PR+, breast cancer cells (Figures 2D and 2E). THZ2 at low

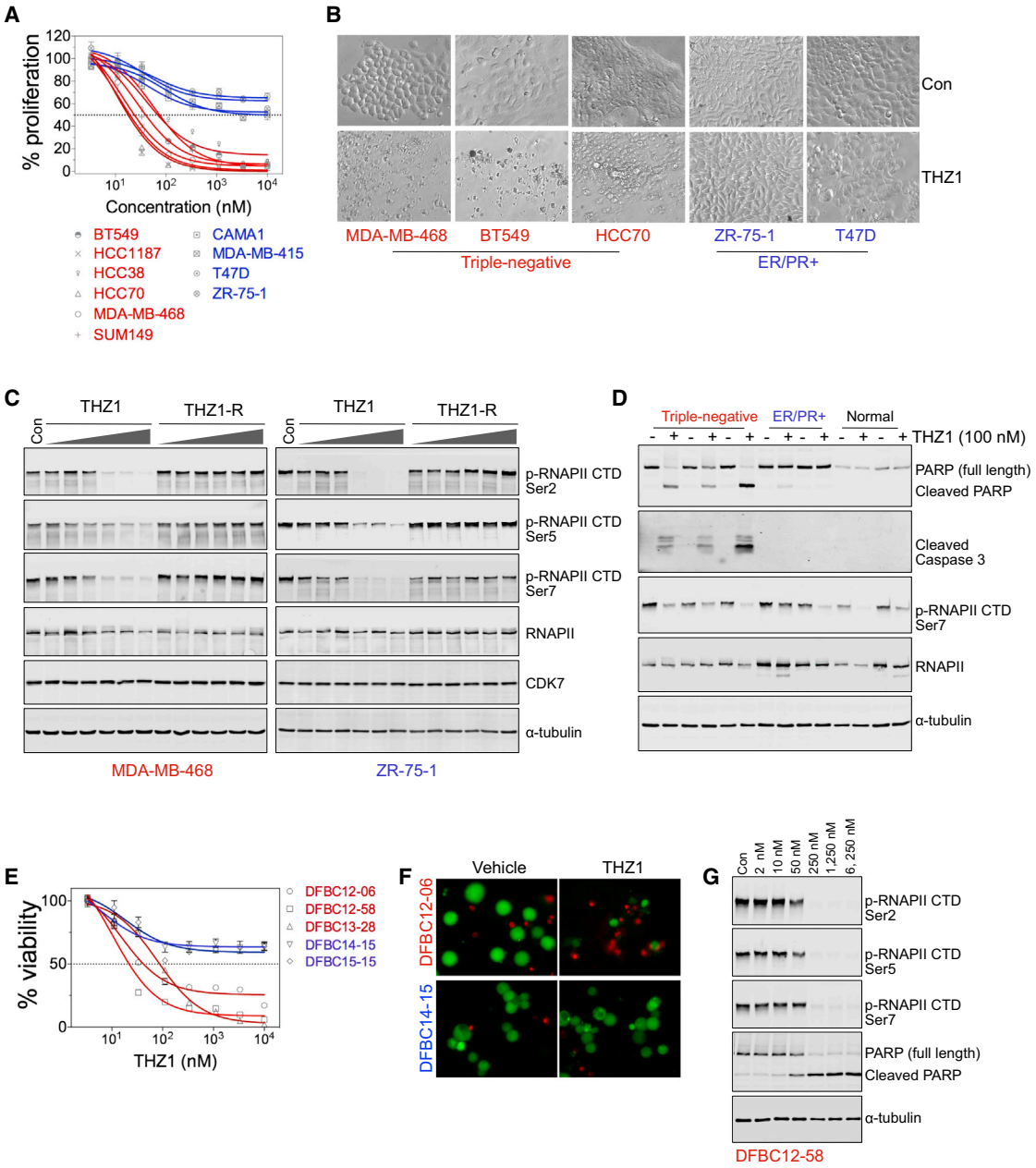

Figure 1. CDK7 Inhibition Selectively Targets TNBC Cells

(A) Cell growth curves of triple-negative (red) and ER/PR+ (blue) breast cancer cell lines. Cells were treated with increasing concentrations of THZ1 for 48 hr. Cells were then fixed and stained for the quantification of cell growth. Data are presented as means ± SD.

(B) Bright-field images of cells that were treated with vehicle control or THZ1 (40 nM) for 7 days. Note that THZ1 induced cell death in triple-negative, but not ER/PR+, breast cancer cells.

(C) THZ1 inhibits RNAPII CTD phosphorylation in both triple-negative (MDA-MB-468) and ER/PR+ (ZR-75-1) breast cancer cells. Cells were treated with vehicle control (first lane) or increasing concentrations of indicated drug (2, 10, 50, 250, 1,250, and 6,250 nM) for 4 hr before lysates were prepared for immunoblotting.

(D) Immunoblotting analysis of lysates harvested from cells treated for 24 hr with vehicle control or THZ1 (100 nM). Samples in the order of loading were triple negative (MDA-MB-468, BT549, HCC1187), ER/PR+ (ZR-75-1, T47D) breast cancer cells, and normal human cells (RPE-1, BJ1).

(E) Indicated TNBC (red) or ER/PR+ (blue) primary cultures were treated with increasing concentrations of THZ1. Cells were subjected to CellTiter-Glow Luminescent Cell Viability Assay after 48 hr of treatment. Data were represented as mean ± SD.

(F) Triple-negative (DFBC12-06) or ER/PR+ (DFBC14-15) primary culture was treated with vehicle control or THZ1 (250 nM) for 24 hr. Cells were subjected to LIVE/DEAD Cell Viability Assay to indicate live (green) and dead (red) cells.

(G) THZ1 inhibits RNAPII CTD phosphorylation and induces apoptosis in primary TNBC cells. Primary TNBC culture (DFBC12-58) was treated with vehicle control (first lane) or indicated concentrations of THZ1 for 24 hr before lysates were prepared for immunoblotting.

See also Figure S1 and Movies S1 and S2.

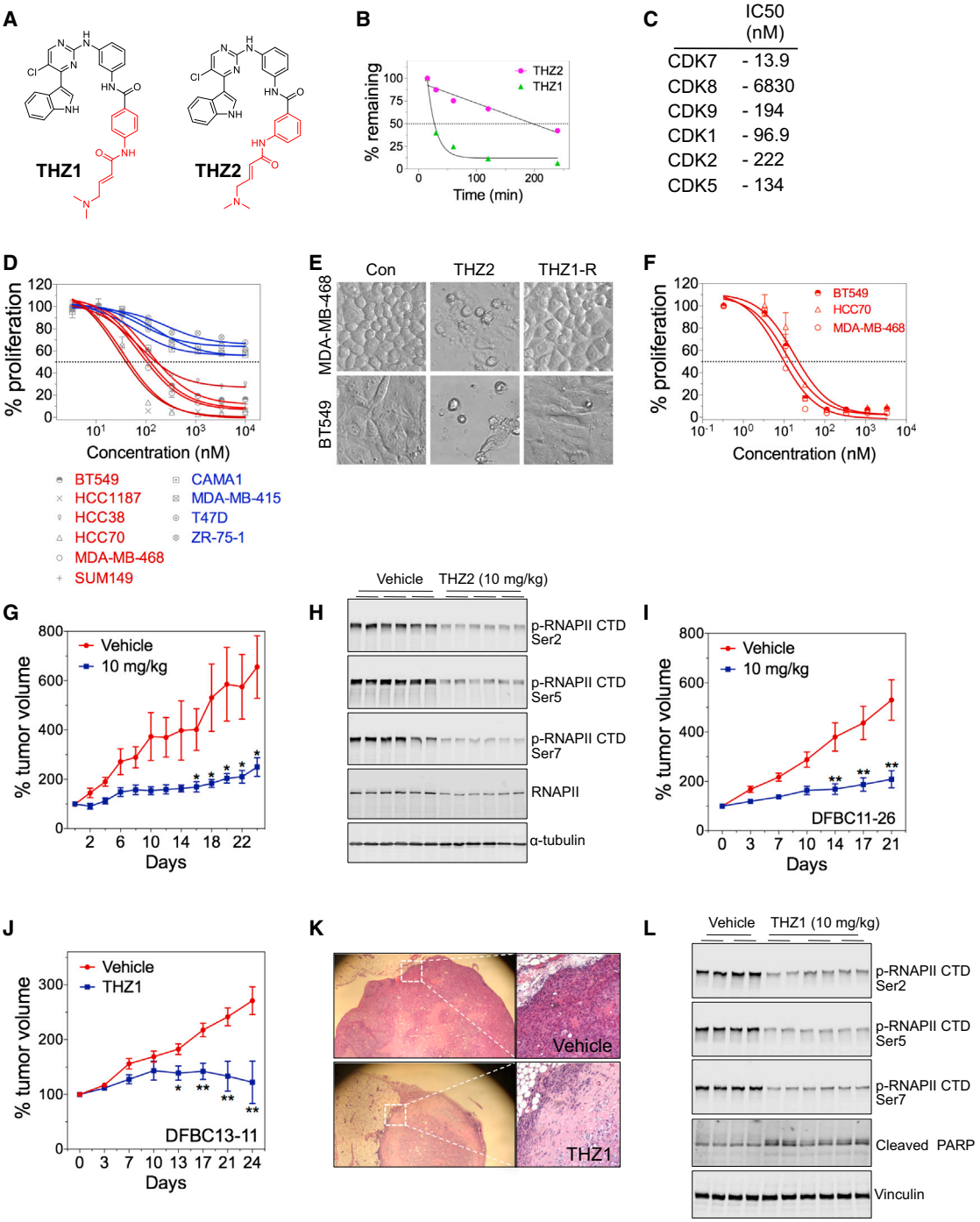

Figure 2. An Analog of THZ1 and the Effect of CDK7 Inhibition on the Growth of Triple-Negative Breast Tumors

(A) Structure of THZ1 and THZ2. The groups of 4-acrylamide-benzamide in THZ1 and 3-acrylamide-benzamide in THZ2 are colored red.

(B) Stability of THZ1 and THZ2 in vivo. Mice were administered by tail vein injection a single dose of THZ1 or THZ2, and blood samples were collected at different time points. Concentrations of THZ1 and THZ2 in plasma samples were determined by liquid chromatography-tandem mass spectrometry (LC-MS/MS) approach.

(C) In vitro IC_{50} for THZ2's potency in binding to indicated CDK. The LanthaScreen Eu Kinase Binding assay (Invitrogen) was performed with indicated CDKs and their associated cyclins in the presence of different concentration of THZ2. The IC_{50} values indicate the affinity of THZ2 toward the ATP binding pocket of CDK.

(D) Cell growth curve of breast cancer cells treated with increasing concentrations of THZ2 for 48 hr. Data are presented as mean ± SD.

(E) Bright-field images of cells treated with vehicle control, THZ2 (370 nM), or THZ1-R (370 nM) for 2 days.

(F) Cell growth curve of indicated TNBC cell lines that were treated with increasing concentrations of THZ2 for 7 days. Upon harvest, cells were fixed and stained with crystal violet, followed by extraction of the staining for the quantification of proliferation. Data are presented as mean ± SD.

(legend continued on next page)

nanomolar doses also efficiently suppressed the clonogenic growth of TNBC cells (IC_{50} of ~10 nM; Figure 2F and S2B). Like THZ1, THZ2 induced apoptotic cell death in triple-negative, but not ER/PR+, breast cancer cells or normal human cells (Figure S2A) and did not cause an obvious alteration in cell cycle (Figure S2C). Therefore, we have identified an analog of THZ2 with improved pharmacokinetic properties and comparable potency that we elected to use for further investigations.

CDK7 Inhibition Suppresses the Growth of Triple-Negative Breast Tumors

We proceeded to investigate whether CDK7 inhibitors would exhibit efficacy in vivo. Treating mice intraperitoneally with THZ2 twice daily at the dose of 10 mg/kg did not give rise to overt toxicity, such as a loss of body weight or behavioral changes (data not shown). To test whether THZ2 has any therapeutic effect on triple-negative breast tumors in an orthotopic xenograft model, we transplanted triple-negative breast tumor cells (MDA-MB-231) into the mammary fat pads of nude mice. When tumors reached ~200 mm^3, mice were treated with vehicle or THZ2 (10 mg/kg). Continuous treatment of THZ2 for 25 days did not affect body weight (Figure S2D), indicating that THZ2 is well tolerated in nude mice. The growth rate of tumors in mice treated with THZ2 was markedly reduced as compared to that of control tumors (Figure 2G), demonstrating an anti-tumor activity of THZ2. We also harvested tumors following short-term (50 hr) or long-term (25 days) treatment and found that both acute and chronic exposure to THZ2 significantly reduced CTD phosphorylation of RNAPII at all three phosphorylation sites (S2, S5, and S7; Figures 2H and S2E), indicating that CDK7 was efficiently targeted in the tumor cells. Compared to vehicle-treated tumors, tumor tissues isolated from mice treated with THZ2 had reduced proliferation and increased apoptosis, as indicated by immunostaining against Ki67 and cleaved Caspase 3, respectively (Figure S2F). Together, these findings indicate that the CDK7 inhibitor was able to efficiently reduce tumor cell proliferation and induce cell death in vivo.

We further evaluated the anti-tumor effect of CDK7 inhibition in two independent PDX models of triple-negative breast tumors, DFBC11-26 and DFBC13-11. Both PDX models were established from patients with metastatic TNBC, who had progressed on multiple lines of chemotherapy. Tumor fragments were transplanted into the mammary fat pads of NOD-SCID mice. Our first experiment with THZ2 in NOD-SCID mice led to reduced body weight, suggesting that THZ2 might be less well-tolerated in this particular mouse strain. We therefore proceeded with using THZ1 in the PDX model of TNBC. When tumors grew to an average size of ~80 mm^3, mice were treated with THZ1. Although THZ1 has poor pharmacokinetic properties, treating mice with this drug led to a substantial blockage of tumor growth in both patient-derived tumor models (Figures 2I and 2J). Notably, THZ1 treatment resulted in a loss of tumor cellularity and disease regression (Figures 2J and 2K). Analysis of tumor tissues also demonstrated markedly decreased CTD phosphorylation of RNAPII and induced PARP cleavage, an indicator of apoptotic cell death (Figure 2L). These results indicate that CDK7 inhibition has potent anti-tumor activity in patient-derived TNBC in vivo.

TNBC Cells Are Highly Dependent on CDK7

To complement the pharmacological studies, which have the potential for unanticipated "off-target" effects, we first used short hairpin RNA (shRNA) to decrease expression of CDK7 in a variety of breast cancer cell lines. Using doxycycline-inducible shRNA vectors targeting multiple independent sequences of CDK7, we were able to reduce the abundance of CDK7 protein by ~20%–50% (Figure S3A). This modest reduction in CDK7 abundance was sufficient to inhibit the growth of triple-negative, but not ER/PR+, breast cancer cells (Figure S3B).

To further corroborate these results, we used the CRISPR/Cas9 technique to genetically edit the CDK7 gene in five TNBC cell lines. Treating cells with constructs encoding two independent small guiding RNA targeting CDK7 (sg_CDK7) led to a substantial reduction of CDK7 protein (Figure S3C) and suppression of cell growth preferentially in triple-negative, but not ER/PR+, breast cancer cells (Figure 3A). Notably, introducing sg_CDK7 strongly impaired tumor formation from orthothopically transplanted TNBC cells (Figure 3B). As observed with the CDK7 inhibitor, sg_CDK7 also induced apoptotic cell death in TNBC cells (Figure 3C) and had little effect on cell-cycle distribution (Figures 3D and S3D). Thus, both shRNA-mediated knockdown of CDK7 and CRISPR/Cas9-mediated CDK7 gene editing produce effects on TNBC cells that phenocopy pharmacologic inhibition of CDK7. These results support the view that CDK7 is the pharmacologically relevant target of the inhibitor and that CDK7 represents a bona fide target for TNBC.

CDK7 Is a Uniquely Important Transcriptional CDK for TNBC

CDK7 is one of the transcriptional CDKs that regulate the initiation or elongation of RNAPII-mediated transcription (Zhou

(G) Growth of triple-negative breast tumors (MDA-MB-231) in nude mice treated with vehicle (n = 8) or THZ2 (n = 7; 10 mg/kg intraperitoneal). Mean ± SEM values are presented; *p < 0.05 (Student's t test).

(H) Immunoblotting of tumor lysates harvested from nude mice treated with vehicle or THZ2 (10 mg/kg intraperitoneal) for 2 days. Tumors were isolated 3 hr after last treatment and subjected to the preparation of RIPA lysates. Three independent samples from each treatment were loaded in duplicates.

(I) Growth of patient-derived triple-negative breast tumors (DFBC11-26) in NOD-SCID mice treated with vehicle (n = 4) or THZ1 (n = 6; 10 mg/kg intraperitoneal). Mean ± SEM values are presented; **p < 0.01 (Student's t test).

(J) Growth of patient-derived triple-negative breast tumors (DFBC13-11) in NOD-SCID mice treated with vehicle (n = 6) or THZ1 (n = 5; 10 mg/kg intraperitoneal). Mean ± SEM values are presented; *p < 0.05 and **p < 0.01 (Student's t test).

(K) H&E staining of tissue sections (DFBC13-11) indicating tumor regression after THZ1 treatment. Note that THZ1-treated tumor shows a loss of cellularity compared to control. Images on the left and right were captured using 4× and 10× object lens, respectively.

(L) Immunoblotting of tumor lysates (DFBC11-26) harvested from mice treated with vehicle or THZ1 (10 mg/kg intraperitoneal) for 21 days. Samples (two and three for vehicle and THZ1 treated groups, respectively) were loaded in duplicates.

See also Figure S2 and Table S1.

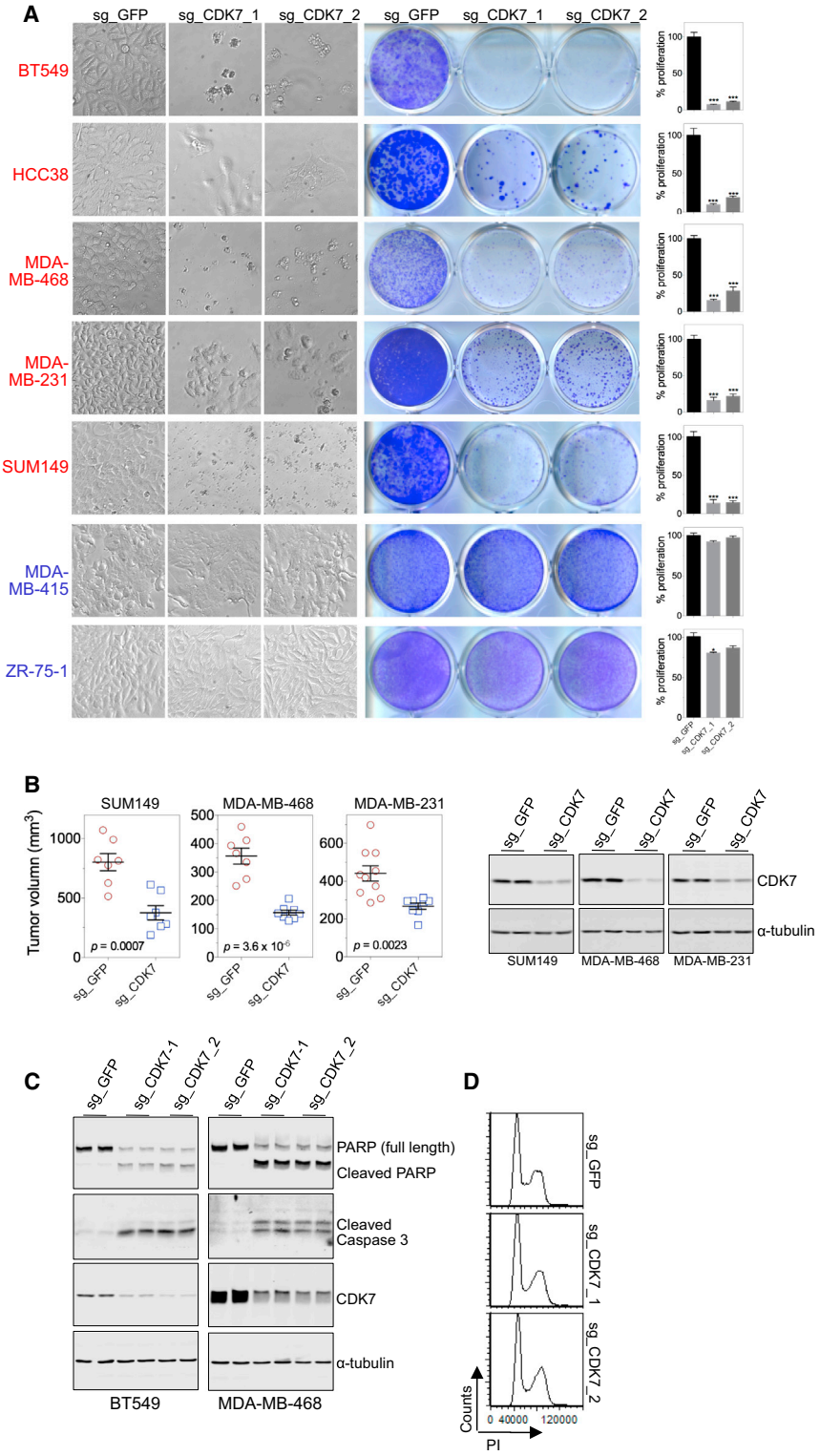

Figure 3. Loss of CDK7 Impairs TNBC Cell Growth and Tumorigenesis

(A) Loss of CDK7 in TNBC cells impairs cell viability and proliferation. The left, middle, and right panels show the bright-field images, the crystal violet staining of cells, and the quantification of cell growth, respectively. Data in the right panel are presented as mean ± SD; *p < 0.01 and ***p < 0.0001 (Student's t test).

(B) Tumor volume of xenografts derived from cells infected with sg_GFP or sg_CDK7 (sg_CDK7_2 in Figure 3A). Cells were infected with lentivirus, selected with puromycin for 2 days, and then harvested for transplantation. Two million MDA-MB-468 or MDA-MB-231 or 4 million SUM149 cells (viability > 94% for all groups, assayed by trypan blue exclusion) were transplanted into mammary fat pads of nude mice. Tumor volume was measured 4 weeks after transplantation for the lines of SUM149 and MDA-MB-231 and 5 weeks for MDA-MB-468. Data were represented as mean ± SEM, with p value indicated. The right panel shows immunoblotting from cultured cells that were used for transplantation. Note that the protein abundance of CDK7 was efficiently decreased by sg_CDK7.

(C) Immunoblotting of lysates from cells introduced with CRISPR constructs. Lentivirus-infected and puromycin-selected cells were seeded in 6-well plate (20, 000 cells per well) and harvested in 4 days. RIPA lysates were subjected to the analysis of apoptotic cell death (indicated by PARP and Caspase 3 cleavage).

(D) Cell-cycle analysis of cells infected with lentivirus encoding sg_GFP, two independent sgRNA targeting CDK7. Cells were prepared as in (C) and then fixed for cell-cycle assay.

See also Figure S3.

et al., 2012). The demonstration of CDK7 as a selective target for TNBC led us to ask if other transcriptional CDKs might also serve as therapeutic targets. We used CRISPR/Cas9 to ablate six known CDKs that are implicated in transcriptional regulation, including CDK7, 8, 9, 12, 13, and 19 (Figures 4A and S4). These studies demonstrated that, like CDK7, CDK9 was also required for clonogenic growth of TNBC cells (MDA-MB-231, MDA-MB-468, and BT549) (Figures 4B and 4C). CDK9 has been implicated in regulating transcriptional elongation, and physiologically, in the differentiation of multiple cell types (Shapiro, 2006). To determine whether CDK9 can also be targeted for TNBC in a selective manner, we further ablated transcriptional CDKs in ER/PR+ breast cancer line (ZR-75-1) (Figure S4). Notably, ER/PR+ breast cancer cells were also sensitive to sg_CDK9 but were largely unaffected by sg_CDK7 (Figures 4C and 4D). Together, these data suggest that, among these transcriptional CDKs, CDK7 is uniquely required for the survival and proliferation of TNBC cells.

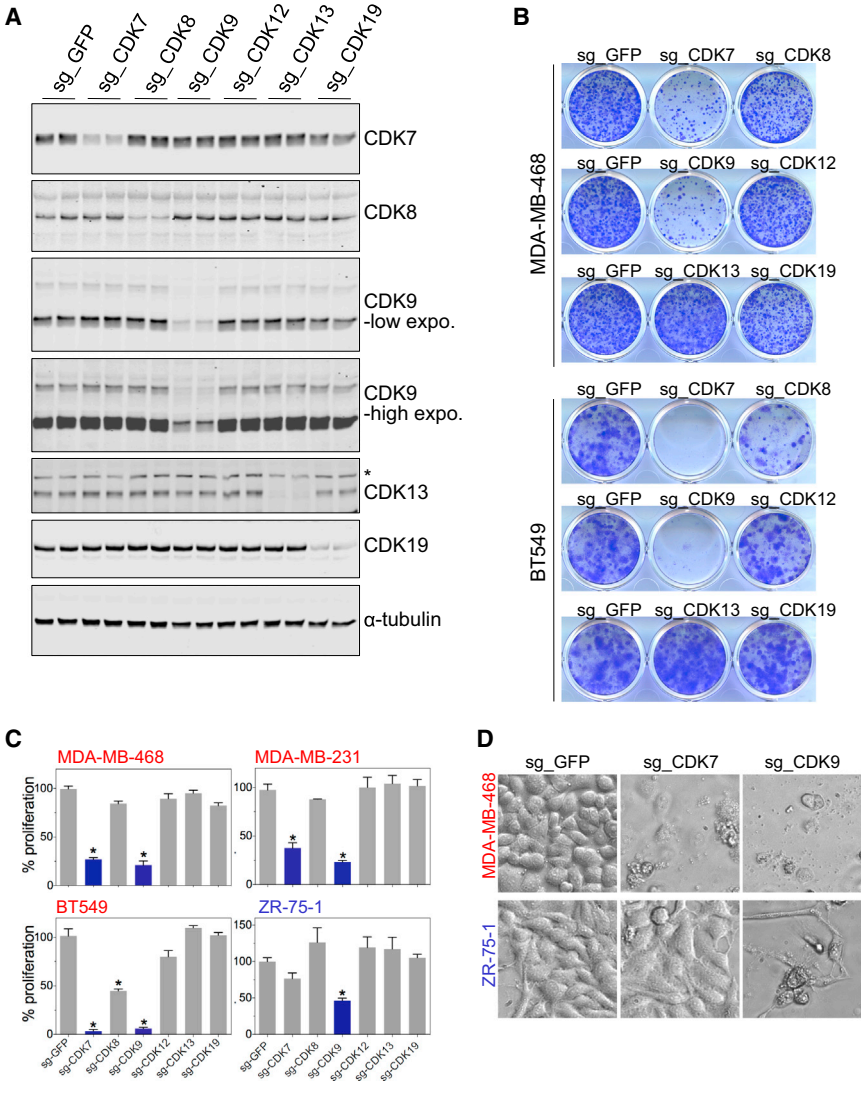

Figure 4. Unique Dependence of TNBC Cells on CDK7

(A) Immunoblotting of lysates from MDA-MB-468 cells that were infected with lentivirus encoding Cas9 and sgRNA targeting GFP or individual transcriptional CDK. The asterisk (*) denotes a non-specific signal for anti-CDK13.

(B) Role of transcriptional CDK for the indicated TNBC cells. After infection and selection with puromycin (1.5 μg/ml, 48 hr), cells were seeded in 12-well plate (5000 per well for MDA-MB-468, 10,000 per well for BT549). Cells were fixed after 11 days and stained with crystal violet.

(C) Quantification of cell proliferation. Cells were treated as in (B). The staining was subsequently extracted for measurement of absorbance to quantify cell growth. Data are presented as mean ± SD; *$p < 0.0001$ (Student's t test).

(D) Bright-field images of cells infected with virus encoding sg_GFP, sg_CDK7 or sg_CDK9. Cells were assayed as in (B) and imaged with an inverted microscope.

See also Figure S4.

CDK7-Dependent Transcription of an "Achilles Cluster" of TNBC Genes

Given the role of CDK7 in phosphorylating the RNAPII CTD and CDK9 at active genes (Drapkin et al., 1996; Glover-Cutter et al., 2009; Akhtar et al., 2009; Larochelle et al., 2012; Kwiatkowski et al., 2014), we expected that CDK7 inhibition would disrupt gene expression. Indeed, THZ1 treatment led to a dose-dependent reduction in steady-state mRNA levels for the tested breast cancer cell lines (Figures 5A and S5A). However, THZ1 treatment affected the proliferation of triple-negative, but not ER/PR+, breast cancer cells. Previous studies with other cancer cell types have shown that THZ1 treatment can cause selective loss of cancer-specific oncogene expression with concurrent loss of tumor cell viability (Kwiatkowski et al., 2014; Chipumuro et al., 2014; Christensen et al., 2014). We therefore hypothesized that a critical set of TNBC genes that are differentially expressed between TNBC and ER/PR+ cells may confer the special sensitivity of TNBC cells to CDK7 inhibition. To test this hypothesis, we first identified genes that are overexpressed in TNBC compared to ER/PR+ breast cancer lines. Genome-wide expression data were generated from two TNBC and two ER/PR+ cell lines over a THZ1 concentration course, and genes were identified that were overexpressed in either TNBC line relative to the ER/PR+ lines. Approximately 1,000 genes were overexpressed in TNBC lines relative to ER/PR+ lines; 451 of these were found to be especially sensitive to treatment with THZ1 (greater than 1.5-fold loss of expression) (Figure 5B).

Gene ontology analysis of the TNBC-specific and THZ1-sensitive genes showed that they were significantly enriched for factors involved in signaling and transcription regulation (Figure 5C). Notably, the genes within these categories included a substantial number of signaling molecules and transcription factors with established roles in breast cancer, including TGFB, STAT, WNT, and EGFR/MET-mediated signaling (Bafico et al., 2004; Brand et al., 2014; Knight et al., 2013; Lu et al., 2014; Pukrop et al., 2006; Truong et al., 2014; Yang et al., 2011) (Figure 5D). Additionally, genes encoding transcription factors whose transcription is regulated by these signaling pathways in breast cancer, including MYC, ETS1, and the epithelial-to-mesenchymal transition-related transcription factors SOX9, TWIST1, and FOXC1, were enriched in this gene set (Guo et al., 2012; Lu et al., 2014; Scheel et al., 2011; Taube et al., 2010; Watabe et al., 1998; Xu et al., 2010; Yang et al., 2004). The majority of these signaling components and transcription factors were commonly expressed in both TNBC cell lines and patient-derived primary cells (Tables S2 and S3A). We thus identified genes showing TNBC-specific expression and sensitivity to THZ1 that encode transcriptional

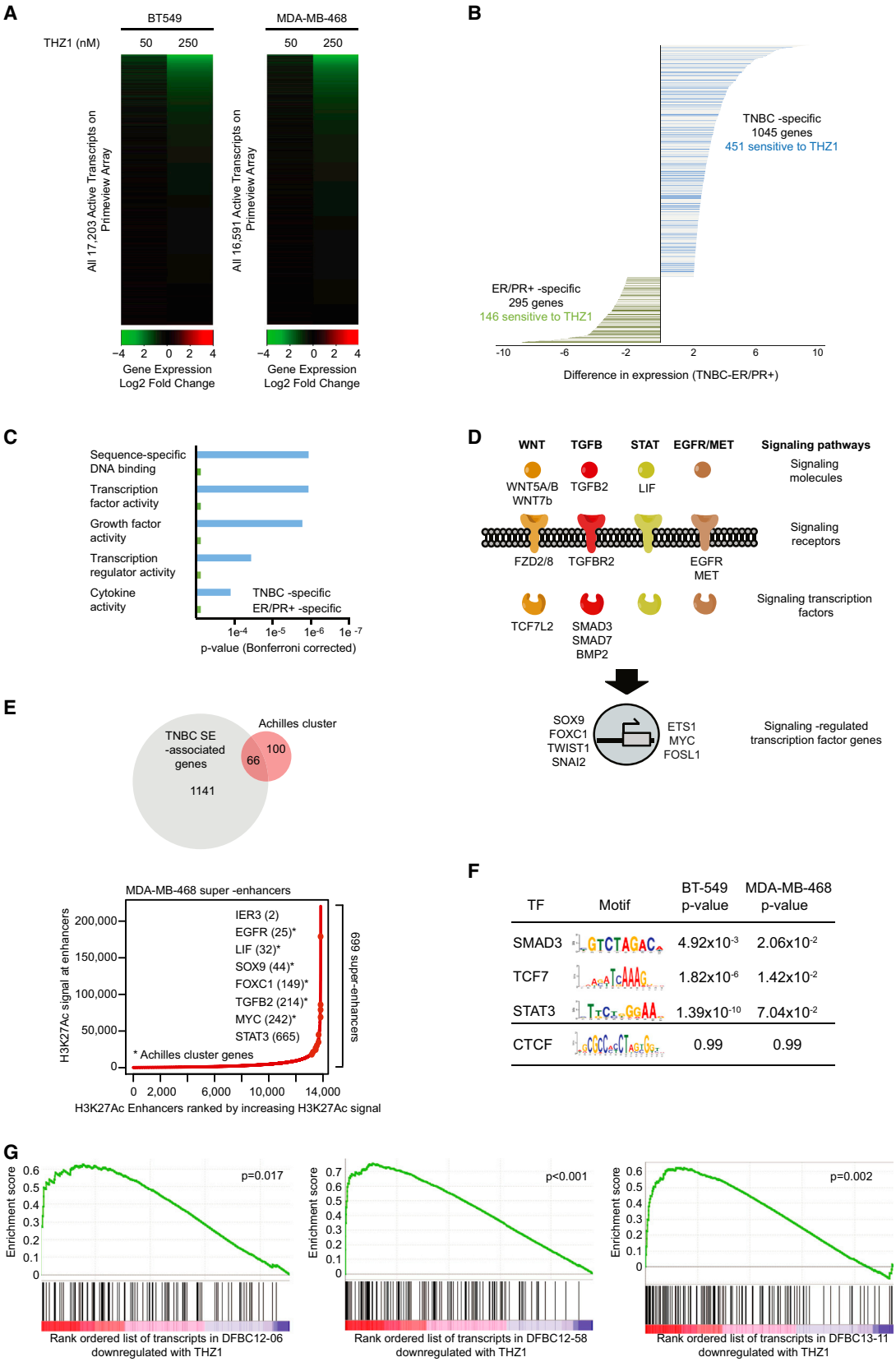

(legend on next page)

regulators and signaling factors, which are candidate mediators of the response to THZ1. This cluster of vital genes encoding transcriptional regulators and signaling factors in TNBC cells may thus collectively represent a TNBC-specific vulnerability—an "Achilles cluster"—for TNBC (Table S3B).

We next sought a mechanistic explanation for the particular sensitivity of Achilles cluster genes to THZ1 treatment and first noticed that 40% of the genes in the Achilles cluster were associated with super-enhancers in TNBC cells. In comparison, only 11% of all expressed genes are associated with super-enhancers in TNBC cells ($p = 8.18 \times 10^{-20}$, chi-square test), and the majority of Achilles cluster genes (83%) are not associated with super-enhancers in ER/PR+ breast cancer cells (Figures 5E, S5B, and S5C and Table S4). Previous work has shown that super-enhancers concentrate components of the transcriptional apparatus to drive high-level expression of their target genes (Hnisz et al., 2013; Lovén et al., 2013; Whyte et al., 2013). Their extraordinary reliance on transcription regulators, including CDK7, may confer special sensitivity to transcriptional inhibitors like THZ1 (Kwiatkowski et al., 2014; Lovén et al., 2013; Chapuy et al., 2013; Chipumuro et al., 2014). Therefore, we hypothesized that the expression of these super-enhancer-associated Achilles cluster genes might be more sensitive to THZ1 than other TNBC genes. Indeed, analysis by microarray expression confirmed that expression of genes associated with super-enhancers in TNBC is particularly sensitive to THZ1 treatment (Figure S5D). Super-enhancers also serve as a platform for regulation by multiple signaling pathways, and perturbation of signaling pathway components can have a profound effect on super-enhancer-associated genes (Hnisz et al., 2015). The super-enhancers associated with genes in the Achilles cluster show a significant enrichment in DNA-binding motifs for terminal effector transcription factors of signaling pathways (Figure 5F). Taken together, these results suggest that the super-enhancer-driven Achilles cluster genes may be sensitive to THZ1 as a result of their dependency on CDK7 and their interconnected regulation by signaling pathways whose components are encoded by genes that are themselves sensitive to THZ1.

We next asked whether THZ1 would induce similar gene expression changes in primary TNBC cells. Gene set enrichment analysis indicated that the genes most sensitive to THZ1 in primary TNBC cells are enriched for the TNBC-specific Achilles cluster genes (Figure 5G). Indeed, quantitative PCR (qPCR) confirmed that, in primary TNBC cultures, the expression of selected TNBC cluster genes was particularly vulnerable to CDK7 inhibition (Figure S5E).

TNBC Cells Are Addicted to the Expression of Achilles Cluster Genes

Next, we sought to confirm that components of the Achilles cluster are essential for TNBC cells and are thus likely to contribute to the cellular response of TNBC cells to CDK7 inhibition. To reflect the composition of the Achilles cluster, we chose eight candidate Achilles cluster genes that encode for super-enhancer-associated transcriptional regulators and signaling factors for this analysis. We used CRISPR/Cas9-mediated gene editing to knock out these candidate genes and assessed how the functional loss of these genes impacts TNBC proliferation and viability. We found that triple-negative (MDA-MB-468, BT549) breast cancer cells were more dependent for proliferation on EGFR, FOSL1, FOXC1, MYC, and SOX9 than ER/PR+ (ZR-75-1) breast cancer cells, while proliferation of the TNBC and ER/PR+ cell lines was similarly sensitive to loss of EN1, ETS1, and TWIST1 (Figures 6A and S6A). Using additional CRISPR vectors that target independent sequences of EGFR or SOX9, we confirmed that gene editing of these two genes suppressed cell growth and induced apoptotic cell death (Figures 6B, 6C, S6B, and S6C).

EGFR has been pursued as a therapeutic target for TNBC (Corkery et al., 2009; Ueno and Zhang, 2011). However, kinase inhibitors of EGFR have not produced satisfactory results in

Figure 5. Genes Expressed Differentially in TNBC versus ER/PR+ Breast Cancer Cells and Sensitive to CDK7 Inhibition Indicate Critical Cellular Functions for TNBC Survival

(A) THZ1 treatment globally affects steady-state mRNA levels. BT549 and MDA-MB-468 TNBC cells were treated with THZ1 at the indicated concentrations for 6 hr. Heatmaps display the Log2 fold change in gene expression versus vehicle control for the set of expressed transcripts.

(B) Genes differentially expressed between TNBC and ER/PR+ breast cancer lines. Individual bars represent the difference in expression in TNBC cells versus ER/PR+ cells for a gene. Genes that were differentially expressed in either of two TNBC cell lines (BT549 and MDA-MB-468) relative to two ER/PR+ lines (ZR-75-1 and T47D) were identified as TNBC specific (right side of y axis). Genes that were differentially expressed in either of two ER/PR+ lines relative to two TNBC breast cancer lines were identified as ER/PR+ specific (left side of y axis). Genes whose expression decreased by 1.5-fold or greater upon treatment with THZ1 were colored (blue for TNBC specific; green for ER/PR+ specific). Log2 fold change between TNBC and ER/PR+ expression is shown along the x axis at the bottom of the image.

(C) Enriched Gene Ontology functional categories of TNBC-specific genes sensitive to THZ1 treatment. The top enriched molecular function GO categories are shown. Individual bars represent the Bonferroni-corrected p value for enrichment of specific gene ontology categories. Values for TNBC-specific, THZ1-sensitive genes are shown in blue. Values for ER/PR+-specific, THZ1-sensitive genes are shown in green.

(D) Depiction of signaling pathways and transcription factors that comprise Achilles cluster genes. Highlighted genes are found in the Achilles cluster.

(E) Achilles cluster genes are enriched in super-enhancers-associated genes. Venn diagram showing the overlap (66) between the genes that comprise the Achilles cluster (166) and genes that have TNBC super-enhancers (SE) in either MDA-MB-468 or BT549 (1207) (top). Total H3K27Ac ChIP-seq signal (length * density) in enhancer regions for all stitched enhancers in MDA-MB-468 TNBC cell line. Enhancers are ranked by increasing H3K27Ac ChIP-seq signal (bottom). Highlighted super-enhancers are associated with selected members of the Achilles cluster. Shown are top super-enhancers for each SE-associated gene.

(F) Enrichment of DNA-binding motifs targeted by signaling transcription factors in constituent enhancers of super-enhancers regulating Achilles cluster genes in TNBC cells. The motif bound by the CTCF transcription factor is not enriched in the super-enhancers associated with Achilles cluster genes and is used as a negative control.

(G) Genes most strongly downregulated by THZ1 treatment in patient-derived TNBC primary cells are enriched for Achilles cluster genes. Gene set enrichment analysis of Achilles cluster genes in comparison to genes downregulated in TNBC primary cultures (DFBC12-06, DFBC12-58, DFBC13-11) following treatment with THZ1 (250 nM) for 6 hr. GSEA-supplied p values are given.

See also Figure S5 and Tables S2, S3, and S4.

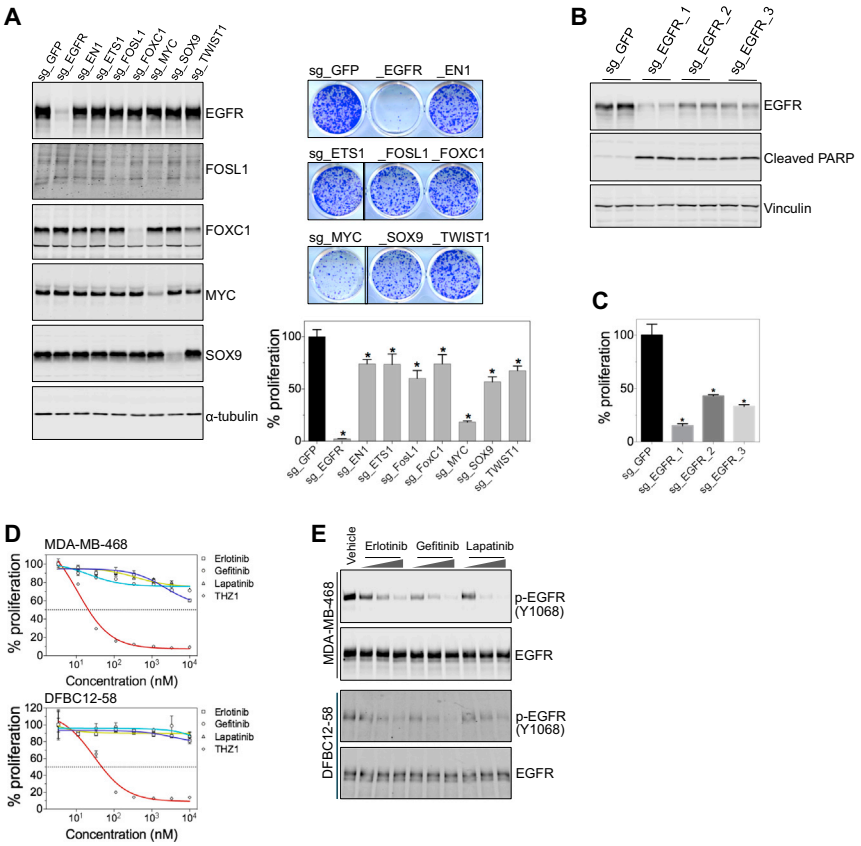

Figure 6. Functions of Achilles Cluster Genes in TNBC Cells

(A) CRISPR/Cas9-mediated editing of selected TNBC Achilles cluster genes in TNBC cell line. MDA-MB-468 cells were infected with lentivirus encoding indicated sgRNA, selected with puromycin. (Left) Immunoblotting for the expression of indicated genes. (Right, top) Cells were seeded in 12-well plates (5,000 cells per well), harvested in 10 days, and stained with crystal violet; the staining was extracted for the quantification of cell growth (right bottom). Data were represented as mean ± SD; *$p < 0.001$.

(B) Additional CRISPR vectors decrease the protein abundance of EGFR. Vectors encoding sg_EGFR_2 and sg_EGFR_3 were tested along with sg_EGFR_1 (sg_EGFR in Figure 6A). Protein lysates were harvested for immunoblotting. Cleaved PARP was used as a marker for apoptotic cell death and Vinculin as a loading control.

(C) CRISPR/Cas9-mediating gene editing of EGFR impairs cell proliferation. MDA-MB-468 cells were treated as in (A) for measurement of cell proliferation, *$p < 0.001$.

(D) Proliferation of TNBC cells (top, MDA-MB-468; bottom, DFBC12-58) treated with increasing concentrations of EGFR inhibitors or THZ1. Cells were harvested in 3 days for measurement of cell proliferation.

(E) TNBC cells (top, MDA-MB-468; bottom, DFBC12-58) were treated with vehicle control or indicated EGFR inhibitors for 30 min. Cell lysates were harvested for immunoblotting.

See also Figure S6.

TNBC clinical trials (Carey et al., 2012). We used three independent kinase inhibitors that are known to target EGFR (erlotinib, gefitinib, and lapatinib) and found that EGFR kinase inhibition largely spared TNBC cells (Figures 6D and S6D), despite evident suppression of EGFR autophosphorylation and downstream MAPK phosphorylation by these inhibitors (Figures 6E and S6E). These data indicate the existence of kinase-independent functions of EGFR that are essential for TNBC cell growth and survival (Weihua et al., 2008) and further suggest that targeting the transcription of EGFR, as achieved by CDK7 inhibition, provides a unique advantage that cannot be achieved by inhibitors of EGFR kinase activity. Together, these data show that targeting CDK7-dependent transcription represents an effective means to collectively suppress the expression of multiple oncogenes that are critical for the proliferation and viability of TNBC cells.

DISCUSSION

Triple-negative breast cancer is a highly aggressive subtype of breast cancer that lacks effective therapeutics, due in part to the genetic complexity that has limited the development of "targeted" therapies. Despite its heterogeneous nature, TNBC cells share a similar transcriptional program, suggesting that tumors of this subtype may be highly dependent on expression of at least a subset of the active genes in these cells. We found that TNBC cells are exceptionally dependent on the transcriptional cyclin-dependent kinase CDK7 and that a cluster of TNBC-specific genes is especially sensitive to CDK7 inhibition. Our results thus indicate that CDK7 mediates transcriptional addiction to this vital cluster of genes in TNBC and that CDK7 inhibition represents a highly promising therapy for this subtype of breast cancer.

CDK7 inhibition revealed an "Achilles cluster" of genes in the TNBC transcriptional program that are likely to be responsible, at least in part, for rendering these cells selectively sensitive to THZ1 treatment. These genes were identified by their overexpression in TNBC cells relative to ER/PR+ cells, their sensitivity to THZ1, and their involvement in transcriptional regulation and in signaling. This group contains putative oncogenes that are misregulated in the triple-negative disease state and essential for TNBC tumorigenicity. For example, loss of transcription factors FOSL1 or SOX9 dramatically impairs the tumorigenic potency of TNBC cells (Tam et al., 2013; Wang et al., 2013) (Figures 6 and S6). Similarly, perturbation of MET- and EGFR-mediated signaling reduces TNBC cell proliferation (Brand et al., 2014; Hsu et al., 2014; Sohn et al., 2014; Figures 6 and S6).

A striking number of genes in the TNBC "Achilles cluster" were associated with super-enhancers in triple-negative, but not in ER/PR+, breast cancer cells, suggesting a mechanism that may contribute to their sensitivity to CDK7 inhibition (Chipumuro et al., 2014; Christensen et al., 2014; Kwiatkowski et al., 2014). Transcription of many of these genes is known to be regulated by signaling pathways whose members are represented in the cluster, and super-enhancers are thought to serve as a platform

for regulation of transcription by signaling pathways. Thus, super-enhancers associated with genes in the Achilles cluster may confer sensitivity to THZ1 by two means: (1) dependency on high levels of transcription apparatus that includes the immediate target of the drug and (2) dependency on a functionally interconnected network of transcription factors and signaling components. Other genes in the cluster do not appear to be associated with super-enhancers, however, so there are likely to be other reasons for their sensitivity to CDK7 inhibition. For example, these genes may depend on continuous expression of some of the super-enhancer-driven transcription factors and may thus be affected secondarily. It is also possible that transcriptional control of this group is more dependent on CDK7 function than others (Kanin et al., 2007), perhaps because they cannot utilize alternative pathways of RNA Pol II CTD phosphorylation, such as that enabled by Erk1/2 (Tee et al., 2014).

The "Achilles cluster" of TNBC genes described here represents a collection of genes encoding transcriptional regulators and signaling components that are overexpressed in multiple TNBC cells and sensitive to CDK7 inhibition, which differs from the well-established approach of seeking a signature for a cancer subtype. Signatures typically include genes that are commonly expressed in cancer subtypes; such signatures are especially valuable when it is likely that a common gene or set of genes must be responsible for a phenotype. In contrast, when the subtype is genetically heterogeneous, we suggest that it is valuable to compile a larger collection of genes (the union of genes in multiple samples, rather than the intersection) that are affected by transcriptional inhibition in multiple cell lines or patient samples concurrent with a cellular phenotype because disregulation of different subsets of the genes in the cluster may produce the same phenotype in a cancer subtype with a complex genotype. The benefit of this approach is the potential to explain how tumor cells that are genetically heterogeneous may be dependent on diverse, yet overlapping, sets of genes.

The strategy of targeting transcription of a cluster of cancer-specific genes, as described here for TNBC, may be applicable to other difficult-to-treat cancers. Recent large-scale efforts have found that TNBC gene expression patterns are highly correlated with aggressive ovarian cancer and lung squamous carcinomas (Cancer Genome Atlas Network, 2012; Hoadley et al., 2014). As with TNBC, these cancers have a high mutation rate, an extremely high prevalence of p53 mutations, and lack a commonly altered genetic event that can be targeted for therapeutic intervention (Cancer Genome Atlas Research Network, 2011, 2012). Thus, it is possible that various aggressive tumors develop transcriptional addictions to clusters of genes that are misregulated and dependent on CDK7, and if so, CDK7 inhibition might be useful therapy for such cancers.

In summary, we have discovered a CDK7-dependent transcriptional addiction in triple-negative breast cancer and identified CDK7 inhibition as a highly selective and potent means to disrupt expression of a key cluster of genes. Our study demonstrates that inhibition of transcription is an effective strategy to target highly aggressive breast cancers with high genetic heterogeneity and lacking obvious "driver" oncogenes. Further studies will be required to determine whether these observations will translate to clinical treatment of human breast cancer.

EXPERIMENTAL PROCEDURES

Cell Culture

Human breast cancer cell lines were grown in RPMI-1640, 10% fetal bovine serum, and 1% penicillin/streptomycin. For gene knockdown assays, cells were infected with lentivirus encoding sgRNA or tetracycline-inducible shRNA. Details of cell culture, construction of plasmids, and viral infection are described in the Supplemental Experimental Procedures.

Animal Studies

All animal experiments were conducted in accordance with the animal use guidelines from the NIH and with protocols approved by the Dana-Farber Cancer Institute Animal Care and Use Committee. Full details are described in the Supplemental Experimental Procedures.

ChIP-Seq and Data Analysis

ChIP was performed as previously described (Lee et al., 2006), using anti-H3K27ac (Abcam, AB4729A). Details of ChIP-seq and data analysis are described in the Supplemental Experimental Procedures. ChIP-Seq and gene expression microarray data are deposited in GEO: GSE69107.

Data Analysis of Gene Expression

To calculate differential expression, Log2 signal intensities were used. For each transcript, the maximum Log2 signal intensity from either of the two ER/PR+ breast cancer cell lines was subtracted from the maximum Log2 signal intensity for that transcript in either of the two TNBC cell lines. Transcripts with a difference of +2 or greater were classified as more expressed in TNBC cells. Transcripts with a difference of −2 or less were classified as more expressed in ER/PR+ breast cancer cells. For sensitivity to THZ1 treatment, transcripts were considered sensitive if the expression level declined greater than 1.5-fold upon treatment with 250 nM THZ1. Any gene with one or more transcripts that passed the two criteria described above was considered for further analysis. For gene ontology analysis, the DAVID suite of online tools (http://david.abcc.ncifcrf.gov/tools.jsp) was used to interrogate the molecular function ontology defined by the Gene Ontology Consortium.

ACCESSION NUMBERS

ChIP-seq and gene expression microarray data are deposited in GEO: GSE69107.

SUPPLEMENTAL INFORMATION

Supplemental Information includes Supplemental Experimental Procedures, six figures, four tables, and two movies and can be found with this article online at http://dx.doi.org/10.1016/j.cell.2015.08.063.

AUTHOR CONTRIBUTIONS

Y.W., T.Z., N.K., R.A.Y., N.S.G., and J.J.Z. conceived the studies. Y.W. and N.K. designed and performed the majority of experiments. T.Z. developed THZ2. B.J.A., N.K., and T.I.L. performed computational analyses. Patient-derived TNBC mouse models were developed by E.L., D.G.S., H.Y., T.V., Z.C.W., and J.D.I. Additional experiments were performed by S.X. (Ion Torrent sequencing), Z.L. (time-lapse image of cells treated with THZ1), and H.L. (cloning of CRISPR-Cas9 constructs targeting CDK7). Y.W., T.Z., N.K., R.A.Y., N.S.G., and J.J.Z. wrote the manuscript with input from all co-authors.

ACKNOWLEDGMENTS

We thank D. Wiederschain and F. Zhang for sharing the plasmids. We thank the Nikon Imaging Center at Harvard Medical School, DFCI Flow Cytometry Core Facility, and Dana-Farber/Harvard Cancer Center Rodent Histopathology Core for technical assistance and the use of instruments. This study was supported by NIH R01CA179483-01 (N.S.G.), a MIT-DFCI Bridge grant (N.S.G. and R.A.Y.), and NIH/NCI P50 CA168504 (J.Z.). N.S.G., T.Z., and

N.K. are inventors on a patent application covering THZ1 and THZ2. N.S.G. and R.A.Y. are scientific founders of Syros Pharmaceuticals, a company that has licensed THZ1 and THZ2 from the Dana-Farber Cancer Institute.

Received: January 22, 2015
Revised: May 27, 2015
Accepted: August 12, 2015
Published: September 24, 2015

REFERENCES

Abramson, V.G., Lehmann, B.D., Ballinger, T.J., and Pietenpol, J.A. (2015). Subtyping of triple-negative breast cancer: implications for therapy. Cancer *121*, 8–16.

Akhtar, M.S., Heidemann, M., Tietjen, J.R., Zhang, D.W., Chapman, R.D., Eick, D., and Ansari, A.Z. (2009). TFIIH kinase places bivalent marks on the carboxy-terminal domain of RNA polymerase II. Mol. Cell *34*, 387–393.

Andre, F., Job, B., Dessen, P., Tordai, A., Michiels, S., Liedtke, C., Richon, C., Yan, K., Wang, B., Vassal, G., et al. (2009). Molecular characterization of breast cancer with high-resolution oligonucleotide comparative genomic hybridization array. Clin. Cancer Res. *15*, 441–451.

Bafico, A., Liu, G., Goldin, L., Harris, V., and Aaronson, S.A. (2004). An autocrine mechanism for constitutive Wnt pathway activation in human cancer cells. Cancer Cell *6*, 497–506.

Brand, T.M., Iida, M., Dunn, E.F., Luthar, N., Kostopoulos, K.T., Corrigan, K.L., Wleklinski, M.J., Yang, D., Wisinski, K.B., Salgia, R., and Wheeler, D.L. (2014). Nuclear epidermal growth factor receptor is a functional molecular target in triple-negative breast cancer. Mol. Cancer Ther. *13*, 1356–1368.

Cancer Genome Atlas Network (2012). Comprehensive molecular portraits of human breast tumours. Nature *490*, 61–70.

Cancer Genome Atlas Research Network (2011). Integrated genomic analyses of ovarian carcinoma. Nature *474*, 609–615.

Cancer Genome Atlas Research Network (2012). Comprehensive genomic characterization of squamous cell lung cancers. Nature *489*, 519–525.

Carey, L.A., Rugo, H.S., Marcom, P.K., Mayer, E.L., Esteva, F.J., Ma, C.X., Liu, M.C., Storniolo, A.M., Rimawi, M.F., Forero-Torres, A., et al. (2012). TBCRC 001: randomized phase II study of cetuximab in combination with carboplatin in stage IV triple-negative breast cancer. J. Clin. Oncol. *30*, 2615–2623.

Chapuy, B., McKeown, M.R., Lin, C.Y., Monti, S., Roemer, M.G., Qi, J., Rahl, P.B., Sun, H.H., Yeda, K.T., Doench, J.G., et al. (2013). Discovery and characterization of super-enhancer-associated dependencies in diffuse large B cell lymphoma. Cancer Cell *24*, 777–790.

Chin, L., Andersen, J.N., and Futreal, P.A. (2011). Cancer genomics: from discovery science to personalized medicine. Nat. Med. *17*, 297–303.

Chipumuro, E., Marco, E., Christensen, C.L., Kwiatkowski, N., Zhang, T., Hatheway, C.M., Abraham, B.J., Sharma, B., Yeung, C., Altabef, A., et al. (2014). CDK7 inhibition suppresses super-enhancer-linked oncogenic transcription in MYCN-driven cancer. Cell *159*, 1126–1139.

Christensen, C.L., Kwiatkowski, N., Abraham, B.J., Carretero, J., Al-Shahrour, F., Zhang, T., Chipumuro, E., Herter-Sprie, G.S., Akbay, E.A., Altabef, A., et al. (2014). Targeting transcriptional addictions in small cell lung cancer with a covalent CDK7 inhibitor. Cancer Cell *26*, 909–922.

Corkery, B., Crown, J., Clynes, M., and O'Donovan, N. (2009). Epidermal growth factor receptor as a potential therapeutic target in triple-negative breast cancer. Ann. Oncol. *20*, 862–867.

Dawson, M.A., Prinjha, R.K., Dittmann, A., Giotopoulos, G., Bantscheff, M., Chan, W.I., Robson, S.C., Chung, C.W., Hopf, C., Savitski, M.M., et al. (2011). Inhibition of BET recruitment to chromatin as an effective treatment for MLL-fusion leukaemia. Nature *478*, 529–533.

Delmore, J.E., Issa, G.C., Lemieux, M.E., Rahl, P.B., Shi, J., Jacobs, H.M., Kastritis, E., Gilpatrick, T., Paranal, R.M., Qi, J., et al. (2011). BET bromodomain inhibition as a therapeutic strategy to target c-Myc. Cell *146*, 904–917.

Drapkin, R., Le Roy, G., Cho, H., Akoulitchev, S., and Reinberg, D. (1996). Human cyclin-dependent kinase-activating kinase exists in three distinct complexes. Proc. Natl. Acad. Sci. USA *93*, 6488–6493.

Fisher, R., Pusztai, L., and Swanton, C. (2013). Cancer heterogeneity: implications for targeted therapeutics. Br. J. Cancer *108*, 479–485.

Gewinner, C., Wang, Z.C., Richardson, A., Teruya-Feldstein, J., Etemadmoghadam, D., Bowtell, D., Barretina, J., Lin, W.M., Rameh, L., Salmena, L., et al. (2009). Evidence that inositol polyphosphate 4-phosphatase type II is a tumor suppressor that inhibits PI3K signaling. Cancer Cell *16*, 115–125.

Glover-Cutter, K., Larochelle, S., Erickson, B., Zhang, C., Shokat, K., Fisher, R.P., and Bentley, D.L. (2009). TFIIH-associated Cdk7 kinase functions in phosphorylation of C-terminal domain Ser7 residues, promoter-proximal pausing, and termination by RNA polymerase II. Mol. Cell. Biol. *29*, 5455–5464.

Guo, W., Keckesova, Z., Donaher, J.L., Shibue, T., Tischler, V., Reinhardt, F., Itzkovitz, S., Noske, A., Zurrer-Hardi, U., Bell, G., et al. (2012). Slug and Sox9 cooperatively determine the mammary stem cell state. Cell *148*, 1015–1028.

Hnisz, D., Abraham, B.J., Lee, T.I., Lau, A., Saint-André, V., Sigova, A.A., Hoke, H.A., and Young, R.A. (2013). Super-enhancers in the control of cell identity and disease. Cell *155*, 934–947.

Hnisz, D., Schuijers, J., Lin, C.Y., Weintraub, A.S., Abraham, B.J., Lee, T.I., Bradner, J.E., and Young, R.A. (2015). Convergence of developmental and oncogenic signaling pathways at transcriptional super-enhancers. Mol. Cell *58*, 362–370.

Hoadley, K.A., Yau, C., Wolf, D.M., Cherniack, A.D., Tamborero, D., Ng, S., Leiserson, M.D., Niu, B., McLellan, M.D., Uzunangelov, V., et al.; Cancer Genome Atlas Research Network (2014). Multiplatform analysis of 12 cancer types reveals molecular classification within and across tissues of origin. Cell *158*, 929–944.

Hsu, Y.H., Yao, J., Chan, L.C., Wu, T.J., Hsu, J.L., Fang, Y.F., Wei, Y., Wu, Y., Huang, W.C., Liu, C.L., et al. (2014). Definition of PKC-α, CDK6, and MET as therapeutic targets in triple-negative breast cancer. Cancer Res. *74*, 4822–4835.

Kanin, E.I., Kipp, R.T., Kung, C., Slattery, M., Viale, A., Hahn, S., Shokat, K.M., and Ansari, A.Z. (2007). Chemical inhibition of the TFIIH-associated kinase Cdk7/Kin28 does not impair global mRNA synthesis. Proc. Natl. Acad. Sci. USA *104*, 5812–5817.

Knight, J.F., Lesurf, R., Zhao, H., Pinnaduwage, D., Davis, R.R., Saleh, S.M., Zuo, D., Naujokas, M.A., Chughtai, N., Herschkowitz, J.I., et al. (2013). Met synergizes with p53 loss to induce mammary tumors that possess features of claudin-low breast cancer. Proc. Natl. Acad. Sci. USA *110*, E1301–E1310.

Kwiatkowski, N., Zhang, T., Rahl, P.B., Abraham, B.J., Reddy, J., Ficarro, S.B., Dastur, A., Amzallag, A., Ramaswamy, S., Tesar, B., et al. (2014). Targeting transcription regulation in cancer with a covalent CDK7 inhibitor. Nature *511*, 616–620.

Larochelle, S., Merrick, K.A., Terret, M.E., Wohlbold, L., Barboza, N.M., Zhang, C., Shokat, K.M., Jallepalli, P.V., and Fisher, R.P. (2007). Requirements for Cdk7 in the assembly of Cdk1/cyclin B and activation of Cdk2 revealed by chemical genetics in human cells. Mol. Cell *25*, 839–850.

Larochelle, S., Amat, R., Glover-Cutter, K., Sansó, M., Zhang, C., Allen, J.J., Shokat, K.M., Bentley, D.L., and Fisher, R.P. (2012). Cyclin-dependent kinase control of the initiation-to-elongation switch of RNA polymerase II. Nat. Struct. Mol. Biol. *19*, 1108–1115.

Lee, T.I., Johnstone, S.E., and Young, R.A. (2006). Chromatin immunoprecipitation and microarray-based analysis of protein location. Nat. Protoc. *1*, 729–748.

Lovén, J., Hoke, H.A., Lin, C.Y., Lau, A., Orlando, D.A., Vakoc, C.R., Bradner, J.E., Lee, T.I., and Young, R.A. (2013). Selective inhibition of tumor oncogenes by disruption of super-enhancers. Cell *153*, 320–334.

Lu, G., Zhang, Q., Huang, Y., Song, J., Tomaino, R., Ehrenberger, T., Lim, E., Liu, W., Bronson, R.T., Bowden, M., et al. (2014a). Phosphorylation of ETS1 by Src family kinases prevents its recognition by the COP1 tumor suppressor. Cancer Cell *26*, 222–234.

Parker, J.S., Mullins, M., Cheang, M.C., Leung, S., Voduc, D., Vickery, T., Davies, S., Fauron, C., He, X., Hu, Z., et al. (2009). Supervised risk predictor of breast cancer based on intrinsic subtypes. J. Clin. Oncol. *27*, 1160–1167.

Perou, C.M., Sørlie, T., Eisen, M.B., van de Rijn, M., Jeffrey, S.S., Rees, C.A., Pollack, J.R., Ross, D.T., Johnsen, H., Akslen, L.A., et al. (2000). Molecular portraits of human breast tumours. Nature *406*, 747–752.

Pukrop, T., Klemm, F., Hagemann, T., Gradl, D., Schulz, M., Siemes, S., Trümper, L., and Binder, C. (2006). Wnt 5a signaling is critical for macrophage-induced invasion of breast cancer cell lines. Proc. Natl. Acad. Sci. USA *103*, 5454–5459.

Schachter, M.M., and Fisher, R.P. (2013). The CDK-activating kinase Cdk7: taking yes for an answer. Cell Cycle *12*, 3239–3240.

Scheel, C., Eaton, E.N., Li, S.H., Chaffer, C.L., Reinhardt, F., Kah, K.J., Bell, G., Guo, W., Rubin, J., Richardson, A.L., and Weinberg, R.A. (2011). Paracrine and autocrine signals induce and maintain mesenchymal and stem cell states in the breast. Cell *145*, 926–940.

Shah, S.P., Roth, A., Goya, R., Oloumi, A., Ha, G., Zhao, Y., Turashvili, G., Ding, J., Tse, K., Haffari, G., et al. (2012). The clonal and mutational evolution spectrum of primary triple-negative breast cancers. Nature *486*, 395–399.

Shapiro, G.I. (2006). Cyclin-dependent kinase pathways as targets for cancer treatment. J. Clin. Oncol. *24*, 1770–1783.

Sohn, J., Liu, S., Parinyanitikul, N., Lee, J., Hortobagyi, G.N., Mills, G.B., Ueno, N.T., and Gonzalez-Angulo, A.M. (2014). cMET Activation and EGFR-Directed Therapy Resistance in Triple-Negative Breast Cancer. J. Cancer *5*, 745–753.

Tam, W.L., Lu, H., Buikhuisen, J., Soh, B.S., Lim, E., Reinhardt, F., Wu, Z.J., Krall, J.A., Bierie, B., Guo, W., et al. (2013). Protein kinase C α is a central signaling node and therapeutic target for breast cancer stem cells. Cancer Cell *24*, 347–364.

Taube, J.H., Herschkowitz, J.I., Komurov, K., Zhou, A.Y., Gupta, S., Yang, J., Hartwell, K., Onder, T.T., Gupta, P.B., Evans, K.W., et al. (2010). Core epithelial-to-mesenchymal transition interactome gene-expression signature is associated with claudin-low and metaplastic breast cancer subtypes. Proc. Natl. Acad. Sci. USA *107*, 15449–15454.

Tee, W.W., Shen, S.S., Oksuz, O., Narendra, V., and Reinberg, D. (2014). Erk1/2 activity promotes chromatin features and RNAPII phosphorylation at developmental promoters in mouse ESCs. Cell *156*, 678–690.

Truong, H.H., Xiong, J., Ghotra, V.P., Nirmala, E., Haazen, L., Le Dévédec, S.E., Balcioğlu, H.E., He, S., Snaar-Jagalska, B.E., Vreugdenhil, E., et al. (2014). β1 integrin inhibition elicits a prometastatic switch through the TGFβ-miR-200-ZEB network in E-cadherin-positive triple-negative breast cancer. Sci. Signal. *7*, ra15.

Ueno, N.T., and Zhang, D. (2011). Targeting EGFR in triple negative breast cancer. J. Cancer *2*, 324–328.

Wang, H., He, L., Ma, F., Regan, M.M., Balk, S.P., Richardson, A.L., and Yuan, X. (2013). SOX9 regulates low density lipoprotein receptor-related protein 6 (LRP6) and T-cell factor 4 (TCF4) expression and Wnt/β-catenin activation in breast cancer. J. Biol. Chem. *288*, 6478–6487.

Watabe, T., Yoshida, K., Shindoh, M., Kaya, M., Fujikawa, K., Sato, H., Seiki, M., Ishii, S., and Fujinaga, K. (1998). The Ets-1 and Ets-2 transcription factors activate the promoters for invasion-associated urokinase and collagenase genes in response to epidermal growth factor. Int. J. Cancer *77*, 128–137.

Weihua, Z., Tsan, R., Huang, W.C., Wu, Q., Chiu, C.H., Fidler, I.J., and Hung, M.C. (2008). Survival of cancer cells is maintained by EGFR independent of its kinase activity. Cancer Cell *13*, 385–393.

Whyte, W.A., Orlando, D.A., Hnisz, D., Abraham, B.J., Lin, C.Y., Kagey, M.H., Rahl, P.B., Lee, T.I., and Young, R.A. (2013). Master transcription factors and mediator establish super-enhancers at key cell identity genes. Cell *153*, 307–319.

Xu, J., Chen, Y., and Olopade, O.I. (2010). MYC and Breast Cancer. Genes Cancer *1*, 629–640.

Yang, J., Mani, S.A., Donaher, J.L., Ramaswamy, S., Itzykson, R.A., Come, C., Savagner, P., Gitelman, I., Richardson, A., and Weinberg, R.A. (2004). Twist, a master regulator of morphogenesis, plays an essential role in tumor metastasis. Cell *117*, 927–939.

Yang, L., Wu, X., Wang, Y., Zhang, K., Wu, J., Yuan, Y.C., Deng, X., Chen, L., Kim, C.C., Lau, S., et al. (2011). FZD7 has a critical role in cell proliferation in triple negative breast cancer. Oncogene *30*, 4437–4446.

Zhou, Q., Li, T., and Price, D.H. (2012). RNA polymerase II elongation control. Annu. Rev. Biochem. *81*, 119–143.

Zuber, J., Shi, J., Wang, E., Rappaport, A.R., Herrmann, H., Sison, E.A., Magoon, D., Qi, J., Blatt, K., Wunderlich, M., et al. (2011). RNAi screen identifies Brd4 as a therapeutic target in acute myeloid leukaemia. Nature *478*, 524–528.